J. Membrane Biol. 89, 269–280 (1986)

The Journal of
Membrane Biology

Phlorizin Binding to Isolated Enterocytes: Membrane Potential and Sodium Dependence

Diego Restrepo and George A. Kimmich
Department of Radiation Biology and Biophysics, School of Medicine and Dentistry, University of Rochester, Rochester, New York 14642

Summary. Phlorizin binding is studied in isolated intestinal epithelial cells of the chick. Cells are ATP depleted to allow extensive manipulation of ionic gradients and membrane potential ($\Delta\psi$). Phlorizin binding is assayed at steady state. Carrier specific phlorizin binding is defined as D-glucose (90 mM) inhibitable binding. Specific binding displays simple Michaelian kinetics as a function of phlorizin, indicating the presence of a single homogeneous binding site. Sodium concentrations and $\Delta\psi$ modify the apparent binding affinity but not the maximum number of binding sites. In contrast, the activation curve as a function of sodium concentrations is sigmoid and the apparent maximum number of binding sites at saturating sodium is phlorizin dependent. The rate of phlorizin association is both $\Delta\psi$ and sodium-concentration dependent. Dissociation is sodium-concentration dependent but not $\Delta\psi$ dependent. Theoretical analysis indicates binding order of substrates is random. In addition, data suggests that the phlorizin/sodium stoichiometry is 2 : 1. The $\Delta\psi$ dependence can be explained by two models: either translocation is the $\Delta\psi$-dependent step and the free carrier is anionic, or sodium binding is the $\Delta\psi$-dependent step.

Key Words cotransport · membrane potential · sodium dependent sugar transport · phlorizin binding

Introduction

It is well established that the transport of glucose in small intestine and kidney is coupled to the transport of sodium. However, the nature of the coupling mechanism is still being explored. In chicken intestine, Kimmich and Randles (1984) have established that the coupling stoichiometry is 2 sodiums to 1 sugar. In a recent study, we have determined that sodium-sugar cotransport in the same preparation involves simultaneous transport of the substrates (rather than a ping-pong mechanism), and we have ruled out several other hypothetical models for sugar transport. We have proposed the terter ordered model with binding order sodium/sugar/sodium (terter NSN) as the simplest model that can explain our experimental data (Restrepo & Kimmich, 1985*a*,*b*).

Analysis of the binding of a competitive inhibitor to a transport system is usually simpler than the analysis of the flux kinetics (Turner & Silverman, 1980). Phlorizin is known to be a high affinity competitive inhibitor for sodium-dependent sugar transport. In rabbit kidney (Aronson, 1978), dog kidney (Turner & Silverman, 1981), and rabbit intestine (Tannenbaum et al., 1977; Toggenburger et al., 1978; Toggenburger, Kessler & Semenza, 1982), the study of phlorizin binding has provided important information about the mechanism of sodium sugar cotransport. Turner and Silverman (1981) using dog kidney cortex have performed the most complete study of steady-state phlorizin binding to date. They conclude that binding of phlorizin to dog renal cortex brush-border membranes is a process involving random binding of one phlorizin and one sodium. This stoichiometry is consistent with recent measurements of sodium-glucose stoichiometry in rabbit brush-border kidney cortex vesicles (Turner & Moran, 1982*b*).

Phlorizin binding has also provided useful information about the coupling mechanism in intestinal tissue. Based on results on the membrane potential dependence of phlorizin binding to intestinal brush-border vesicles of the rabbit, Toggenburger et al. (1982) have postulated an ordered model with a negatively charged free carrier as the possible mechanistic basis for sodium-sugar cotransport. However, Toggenburger et al. could not carry out a complete kinetic analysis of phlorizin binding at steady state due to a large amount of nonspecific binding and because of difficulty in maintaining diffusion potentials for the length of time required to attain steady-state phlorizin binding. As explained in an earlier publication (Restrepo & Kimmich, 1985*b*), the terter NSN model proposed by us for sodium sugar cotransport in small intestine can also provide a mechanistic basis for explaining the phlorizin binding data of Toggenburger et al. (1982).

Table 1. Composition of the media

Media	Mannitol	Na^+	TMA^+	K^+	Gluconate	NO_3
I	100		150	100	250	
II	100	150	100			250
III	100	50	200			250
IV	100			500	500	
V	100	500				500
VI	100		500			500
VII	100	150	100			250
VIII	100	150		100	250	
IX				250		
X		300				300
XI			300			300
XII		150		150	300	
XIII	100	300	150			450
XIV	100	300		150	450	
XV	100		450			450

All concentrations are in mM.

In this study, we carry out a complete kinetic analysis of phlorizin binding to ATP-depleted chicken intestinal cells. The results allow us to test our proposed model and to provide firmer ground for comparing the chicken intestinal transporter to the kidney cortex transporter and to the rabbit intestinal transporter.

Materials and Methods

Cell Isolation and ATP Depletion

Chick intestinal villi cells were isolated using the hyaluronidase digestion procedure described earlier (Kimmich, 1970). After isolation, cells were washed once in ice-cold isolation media and were ATP depleted by incubation with 80 μM rotenone and 200 μM ouabain (Carter-Su & Kimmich, 1979). De-energized cells were placed on ice and used within 2 hr.

Cells were isolated in solutions of different osmolarities ranging from 500 to 1200 mosM. All solutions had 25 mM HEPES-Tris[1] (pH 7.4 at 37°C), 1 mM $CaCl_2$, 1 mM $MgCl_2$, 1 mg/ml BSA (bovine serum albumin; Sigma fraction V) plus salts and mannitol as indicated in Table 1. Protein was measured employing the biuret method (Gornall, Bardawill & David, 1979).

Phlorizin Binding Assay (Steady State)

Steady-state phlorizin binding was assayed at 37°C. Ninety μl of prewarmed radioactive solution were placed at the bottom of a miniscintillation vial (Starstedt) and 10 μl of cells (20–60 mg cell protein/ml) were placed on the opposite side of the vial. Binding was started by mixing the solutions quickly by vortexing for 6 sec. Unless otherwise specified, the reaction was stopped after 15 sec by adding 5 ml of ice-cold stop solution. Measurements with a YSI tele-thermometer indicated that the temperature of the solution stayed within 2 degrees of 37°C. Cells were immediately centrifuged for 10 sec at 8000 × g in an Adams MHCT table top centrifuge. The cell pellets were dried and washed again with 5 ml of stop media. The entire wash procedure required 30–40 sec. For each individual experiment, measurements were done in triplicate.

The ice-cold stop media contained 25 mM HEPES-Tris, 1 mM $CaCl_2$, 1 mM $MgCl_2$, 1 mg/ml BSA and enough NaCl to make the solution isosmolar with the incubation solution (NaCl concentrations were always larger than 300 mM). The rate of phlorizin dissociation from cells homogeneously suspended in ice-cold stop solution containing 300 mM sodium was -0.29 ± 0.03 min^{-1} (mean ± SD $n = 3$). However, we found that once the cells are centrifuged to a pellet (less than 10 sec) diffusion of phlorizin from the pellet is slow (the ratio of the amount of glucose-inhibitable phlorizin binding measured after the two washes to that measured after the initial 10-sec centrifugation was 1.03 ± 0.04 mean ± SD from three experiments). Since the second wash lowered the background binding by twofold without measurable loss of glucose inhibitable phlorizin binding, the two-wash procedure was used. Addition of phlorizin (30 μM) to the stop solution did not modify the results. Hence, the procedure resulted in retention of more than 95% of the bound phlorizin.

Measurement of Association and Dissociation Rates

As shown in the results, phlorizin binding at 37°C reaches steady state within less than 7 sec. In preliminary experiments we found that dissociation at 37°C is complete in less than 30 sec. Since measurement of rates of association and dissociation under these conditions would be impractical, all measurements of rates were performed at 1–2°C. The stop solution used was the same as in the steady-state experiments with phlorizin (30 μM) added.

Dissociation

Cells were isolated in a solution containing (in mM) 150 K-gluconate, 150 TMA-gluconate, 100 mannitol plus divalent cation salts, buffer and BSA. Cells were de-energized by incubation for 10 min with 80 μM rotenone, 200 μM ouabain, and 40 μg/ml valinomycin. Phlorizin was bound at 37°C using the standard technique to assay phlorizin binding at steady state. The solution used for this purpose contained (final concentrations in mM): 270 $NaNO_3$, 100 mannitol, 15 TMA-gluconate, 15 K-gluconate, 900 μM phloretin, 0.1 μM radioactive phlorizin plus rotenone, valinomycin, and ouabain. At this phlorizin concentration, more than 93% of the total phlorizin bound can be prevented from binding by addition of 90 mM D-glucose. Debinding was initiated by adding 5 ml of ice-cold debinding medium to the 100 μl of cells to which the tritiated phlorizin was bound. The incubation vials were placed on ice and centrifugation (10 sec) was started at different times. In each run, one sample was centrifuged immediately (Bo) and another sample was centrifuged after six min at 37°C (B_{oo}). B was taken as nonspecific binding and trapping and was subtracted from all experimental values for that run. Results were normalized by dividing each value by $Bo - B$. All debinding solutions contained 30 μM unlabeled phlorizin.

[1] N-2-hydroxyethylpiperazine-N'-2-ethanesulfonic acid (Sigma Chemical).

Association

Cells were isolated in a medium containing in mM: 100 mannitol, 300 TMACl, 150 KCl plus buffer, divalent cation salts, and BSA. After isolation, 80 μM rotenone, 200 μM ouabain, and 40 μg/ml valinomycin were added. Binding was assayed with the same procedure used to assay binding at 37°C except that all steps were carried out at 1–2°C and that the wash media contained 30 μM unlabeled phlorizin. The binding rate, in the presence of 270 mM Na^+ and a negative $\Delta\psi$ ranged from 0.1 to 0.5 pmol · mg^{-1} · min^{-1} in different experiments. Data were normalized as follows: Since the zero-time intercept was the same for the different cases (*see* Fig. 10*b*), this was taken as trapping or nonspecific binding and was subtracted from all data. The data at 270 mM Na^+ and negative $\Delta\psi$ was fit to $B = B_i(1 - e^{-\alpha t})$ where t is time and α and B_i are fit parameters. The calculated value for B at 1.2 min was then set to 1 by multiplying by a factor f. All data points in the experiment were then normalized by multiplying by f.

Tritiated phlorizin (57.2 Ci/mmol) was purchased from New England Nuclear (Boston, Mass).

Results

Time Course of Phlorizin Binding To ATP-Depleted Chick Enterocytes

When phlorizin binding (5 μM) to isolated intestinal cells is assayed in the presence of a sodium gradient (Fig. 1*a*), about 50% of the binding can be inhibited by addition of 90 mM D-glucose (addition of 180 mM D-glucose yields the same result). When the D-glucose-inhibitable binding (specific binding) is plotted *vs.* time (Fig. 1*b*), it is clear that steady-state binding is attained in less than 6 sec and that the amount bound is constant for a period of 6 to 60 sec. The results of this experiment at low phlorizin (0.095 μM) are similar except that nonspecific binding is a smaller percentage of total binding (data not shown).

Phlorizin Concentration Dependence of Phlorizin Binding

In order to evaluate the concentration dependence for the specific binding process, the amount of phlorizin bound after a 15-sec interval ± 90 mM D-glucose was assayed. Because it was important to reduce nonspecific binding, we also tested the effect of phloretin, the aglycone of phlorizin, which is a structural analog of phlorizin but which does not inhibit the Na^+-dependent sugar transport system. Table 2 shows that addition of 900 μM phloretin lowers nonspecific binding by a factor of two without modifying carrier specific binding. For this reason, phloretin was included in most subsequent experiments relating to the binding kinetics of phlorizin.

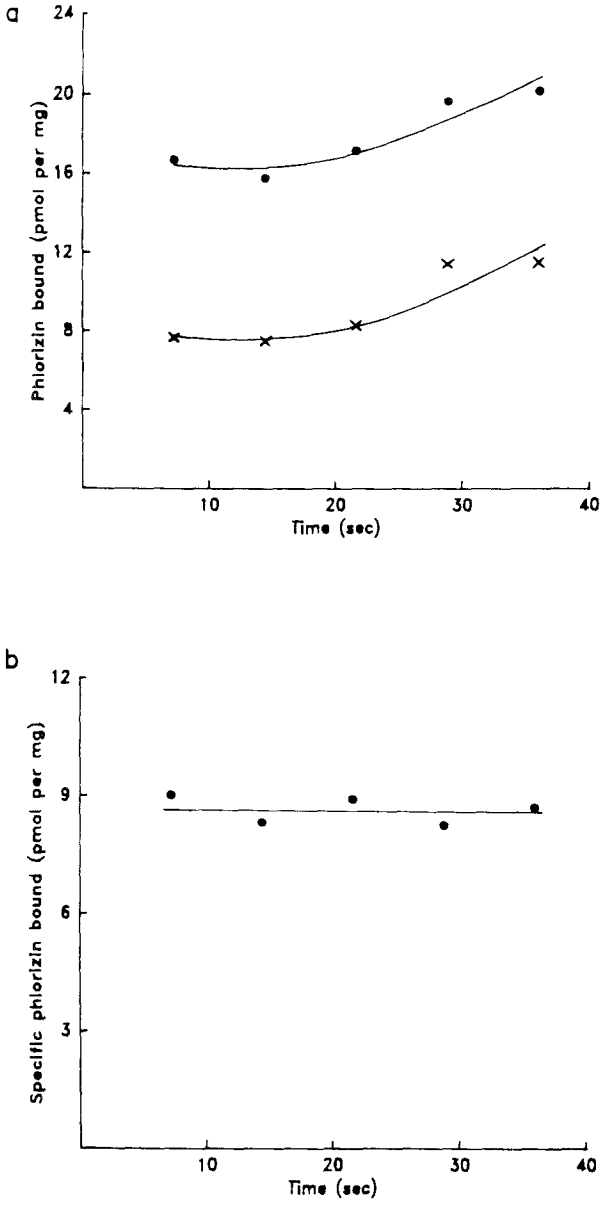

Fig. 1. Time course of phlorizin binding to isolated villi cells. Cells were isolated in solution I and de-energized by preincubation with rotenone and ouabain. At the start of each binding assay, cells were diluted 1 : 10 in medium II which contains 150 mM sodium. A negative-inside diffusion potential was created with a 10-fold potassium gradient plus 40 μg/ml valinomycin. After dilution, the assay medium contained 5 μM radioactive phlorizin. (*a*) Total phlorizin binding plus (x) or minus (●) 90 mM D-glucose (replacing mannitol). (*b*) The D-glucose inhibitable portion of phlorizin binding (specific binding)

Figure 2*a* displays the results of a typical experiment in which the phlorizin concentration dependence of phlorizin binding is studied at a fixed extra-

Table 2. Effect of phloretin on phlorizin binding

Phloretin (μM)	Phlorizin (μM)	Specific binding		Nonspecific binding		n
		pmol/mg	Normalized	pmol/mg	Normalized	
0	0.2	2.53 ± 0.78	1.00	0.41 ± 0.13	0.17 ± 0.04	3
900	0.2	2.65 ± 0.85	1.05 ± 0.07	0.24 ± 0.10	0.10 ± 0.03	3
0	4.0	3.97	1.00	5.21	1.31	1
900	4.0	3.94	0.99	2.53	0.64	1

Measurements were done using de-energized cells in the presence of a negative membrane potential (created using a 10-fold potassium gradient and 40 μg/ml valinomycin) and 135 mM extracellular sodium. Values shown are means ± SD. Specific binding defined as D-glucose-inhibitable (90 mM) phlorizin binding. Amounts were normalized in each experiment to the control specific binding.

Table 3. Effect of different extracellular cations on D-glucose-inhibitable phlorizin binding (specific binding)

Extracellular cation (135 mM)	Specific binding (normalized)
Sodium	1.00
TMA^+	0.019 ± 0.008
Lithium	0.056 ± 0.030
Potassium	0.017 ± 0.009
Trizma	0.023 ± 0.015

Measurements were done using de-energized cells in the presence of a negative membrane potential created using a 10-fold potassium gradient and 40 μg/ml valinomycin (except in the presence of extracellular potassium when the potential was zero). Phlorizin concentration was 0.2 μM. Values were normalized in each experiment to the specific binding in the presence of sodium. The average specific binding in the presence of sodium was 2.53 ± 0.78 pmol/mg. All values are mean ± SD.

cellular sodium concentration and an interior negative membrane potential. As shown, the nonspecific component of phlorizin binding does not saturate in the range of 0–18 μM phlorizin. On the other hand, Fig. 2*b* shows that specific phlorizin binding saturates and that the data can be fit by a rectangular hyperbola [Eq. (1)].

$$B = BmP/(K_{mp} + P) \quad (1)$$

where B is bound phlorizin, P is the extracellular concentration of phlorizin and K_{mp} is the apparent affinity constant. The maximum number of binding sites (Bm) was found to be 10 ± 3 pmol per mg of cellular protein (mean ± SD, n = 8, range: 6.5–15.7). This translates to 6 million binding sites per cell (using an estimated 10^6 cells per mg of protein (Kimmich, 1970)). The apparent binding constant (K_{mp}) under these conditions exhibited considerable variability from experiment to experiment: 1.60 ± 0.63 μM (mean ± SD, n = 8, range: 0.9–2.6 μM).

Cation Dependence of Specific Phlorizin Binding

Table 3 shows that phlorizin binding is highly dependent on the presence of extracellular sodium. Replacing sodium by other cations inhibits more than 95% of the specific phlorizin binding. Sodium increased the affinity of phlorizin binding without modifying the number of binding sites as shown in Fig. 3.

Sodium Activation of Specific Phlorizin Binding

The sodium dependence of specific phlorizin binding was investigated at a fixed inside-negative membrane potential (using potassium plus valinomycin). Figure 4 shows the results of these experiments for two phlorizin concentrations: 0.095 and 0.9 μM. As shown in Fig. 4*b* and *c*, the data cannot be fit by a straight line in a Scatchard plot, but can be linearized when plotted in a modified Scatchard plot where a Hill coefficient for sodium of 1.6 is used [the Hill coefficient n is defined in Eq. (2)]. The binding level reached at saturating sodium concentrations is phlorizin dependent.

$$B = BmnN^n/(N^n + Km^n). \quad (2)$$

In the same set of experiments, the absolute maximum number of binding sites Bm was determined by measuring binding of phlorizin at 135 mM sodium and 15 μM phlorizin and correcting for the degree of saturation achieved at those substrate concentrations using the average value for K_{mp} reported above. Figure 5 shows that when the binding level reached at saturating sodium concentrations found at the two different phlorizin concentrations in Fig. 4*b* and *c* and the maximum number of bind-

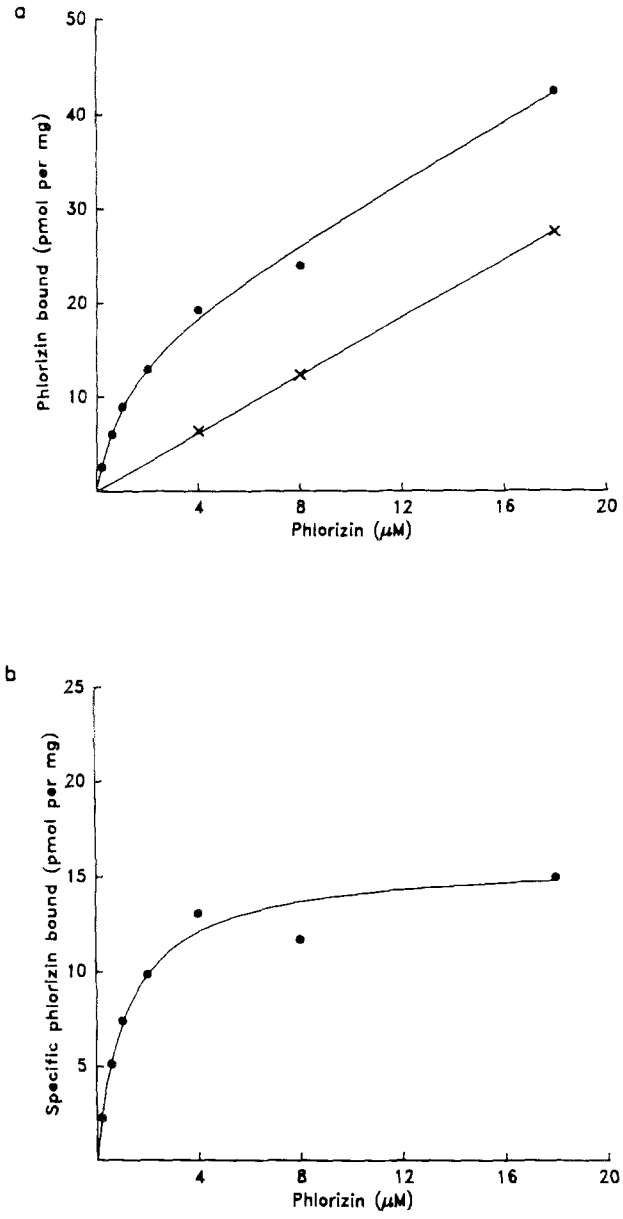

Fig. 2. Phlorizin concentration dependence of phlorizin binding. Cells were isolated in medium I and de-energized. To initiate each binding assay, cells were diluted 1 : 10 into medium II (150 mM sodium) containing radioactive phlorizin (0.22–20 μM) and 1 mM phloretin. An inside-negative diffusion potential was created using a potassium gradient plus 40 μg/ml valinomycin. (*a*) Total phlorizin binding in the presence (x) or absence (●) of 90 mM D-glucose. (*b*) Specific binding. The curve shown in *b* is the best fit of Eq. (1) to the data. The fit parameters are Bm = 15.67 pmol/mg and K_{mp} = 1.20 μM. The nonspecific binding was fit by B = (1.53)P where B is expressed in pmol/mg and P in μM

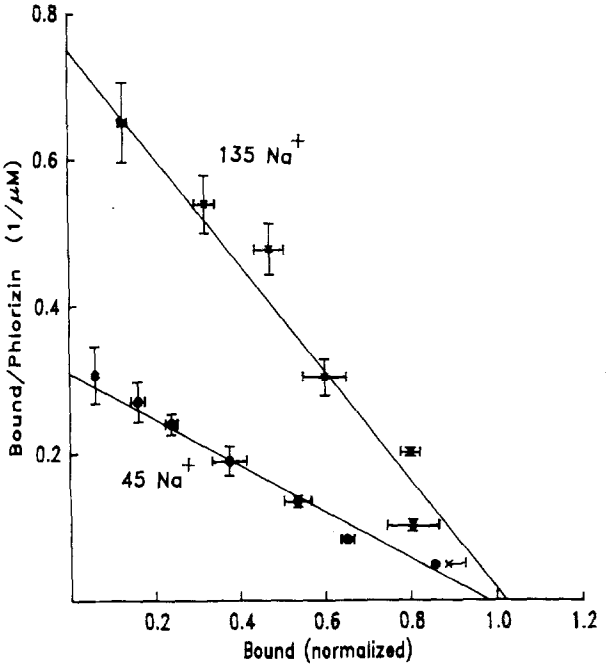

Fig. 3. Scatchard plot of phlorizin binding as a function of phlorizin at two different sodium concentrations. Cells were isolated and diluted as in Fig. 2 except final extracellular sodium concentrations were in mM either 135 (x) or 45 (●) (replaced by TMA^+). The data have been corrected for nonspecific binding by subtracting binding in the presence of 90 mM D-glucose. The results are the average from four experiments ± SEM, n = 4. Data from each experiment were normalized to the average maximum binding found by Scatchard analysis of the data at 135 and 45 mM sodium. The average Scatchard parameters are: at 135 mM sodium, K_{mp} = 1.36 ± 0.22 μM, Bm = 11.36 ± 2.98 pmol/mg; and at 45 mM sodium, K_{mp} = 3.18 ± 0.78 μM, Bm = 10.90 ± 2.89 pmol/mg. The average ratio of Bm(45 mM Na)/Bm(135 mM Na) = 0.96 ± 0.09 and the ratio of $K_{mp}(45)/K_{mp}(135)$ = 2.44 ± 0.65 (all values are mean ± SD, n = 4)

ing sites are plotted in a Scatchard plot, the points fall on a straight line. The significance of this is discussed later.

The dependence of K_{mp} on sodium can be displayed by calculating K_{mp} using Eq. (3)

$$K_{mp} = P((Bm/B) - 1). \quad (3)$$

An internal check for consistency is provided by the fact that when K_{mp} found by this procedure is plotted *vs.* sodium concentration, the result should be the same regardless of the phlorizin concentration at which the data was gathered. Figure 6 shows that this prediction is fulfilled whether K_{mp} is calculated using the data gathered at 0.095 or 0.9 μM phlorizin.

Membrane Potential Dependence of Specific Phlorizin Binding

Figure 7 shows that the apparent affinity constant for phlorizin is altered by changing the membrane

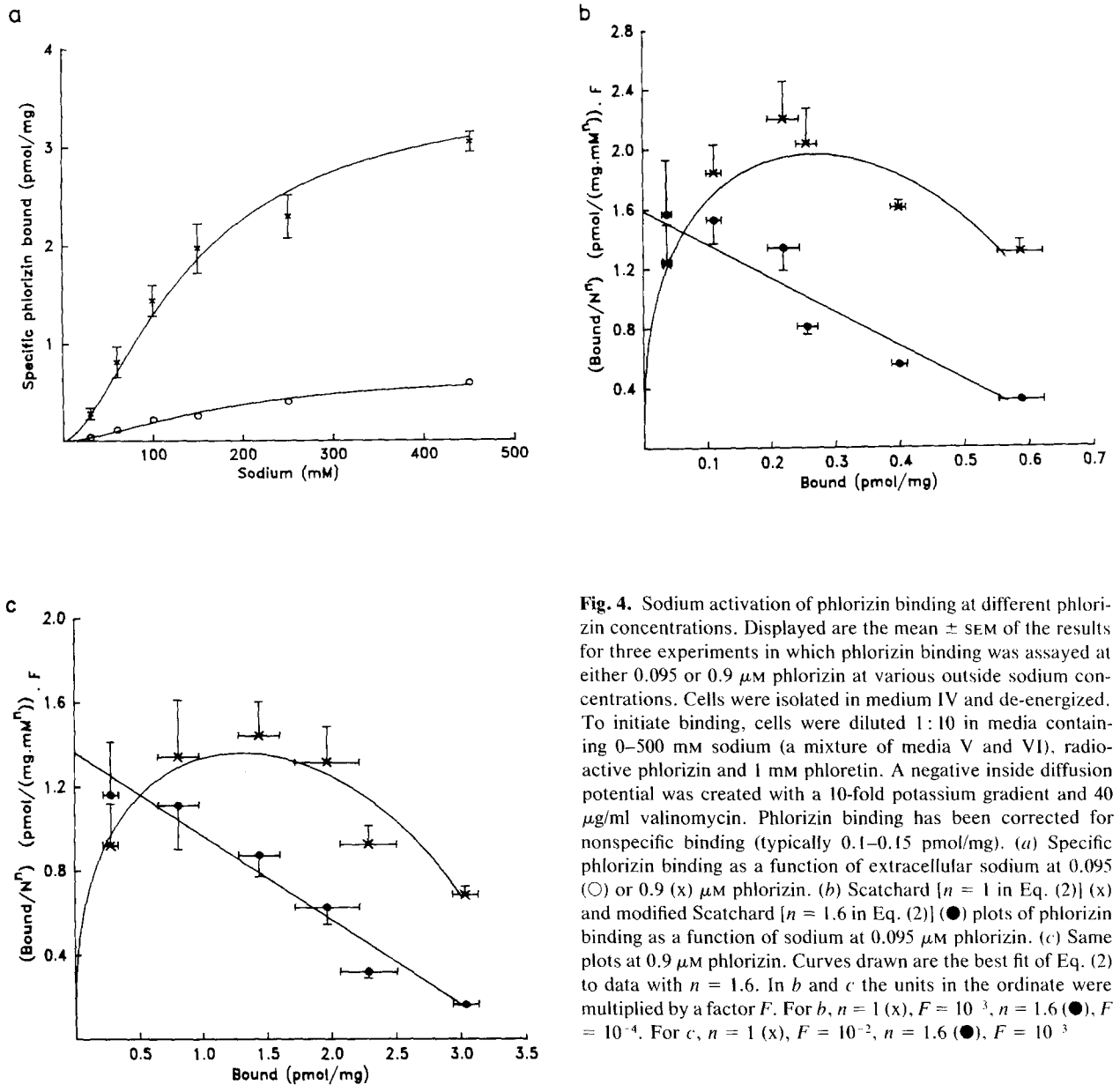

Fig. 4. Sodium activation of phlorizin binding at different phlorizin concentrations. Displayed are the mean ± SEM of the results for three experiments in which phlorizin binding was assayed at either 0.095 or 0.9 μM phlorizin at various outside sodium concentrations. Cells were isolated in medium IV and de-energized. To initiate binding, cells were diluted 1 : 10 in media containing 0–500 mM sodium (a mixture of media V and VI), radioactive phlorizin and 1 mM phloretin. A negative inside diffusion potential was created with a 10-fold potassium gradient and 40 μg/ml valinomycin. Phlorizin binding has been corrected for nonspecific binding (typically 0.1–0.15 pmol/mg). (*a*) Specific phlorizin binding as a function of extracellular sodium at 0.095 (○) or 0.9 (x) μM phlorizin. (*b*) Scatchard [n = 1 in Eq. (2)] (x) and modified Scatchard [n = 1.6 in Eq. (2)] (●) plots of phlorizin binding as a function of sodium at 0.095 μM phlorizin. (*c*) Same plots at 0.9 μM phlorizin. Curves drawn are the best fit of Eq. (2) to data with n = 1.6. In *b* and *c* the units in the ordinate were multiplied by a factor F. For *b*, n = 1 (x), $F = 10^{-3}$, n = 1.6 (●), $F = 10^{-4}$. For *c*, n = 1 (x), $F = 10^{-2}$, n = 1.6 (●), $F = 10^{-3}$

potential. The membrane potential does not change the maximum number of binding sites.

Specificity of Sugar Inhibition of Phlorizin Binding. Ionic Strength and Osmolarity Effects

Figure 8 shows the effect of various sugars on the magnitude of specific phlorizin binding. Actively transported sugars [galactose, α and β methylglucosides and 3-O-methylglucose (Crane, 1960; Kimmich & Randles, 1981)] all inhibit specific phlorizin binding to a greater extent than sugars which are not transported by the Na^+-independent carrier [2-deoxyglucose and D-mannose (Crane, 1960; Kimmich & Randles, 1976)].

Figure 8 also shows that changing the osmolarity of the outside media from 532 to 1151 mosM does not alter specific binding significantly. In previous experiments we have determined that intracellular volumes change in response to osmolarity in less than 10 sec (data not shown). The lack of osmotic effects on cellular phlorizin indicates that phlorizin is bound rather than accumulated inside the cells. The figure also shows that there is no effect of changing the ionic strength (I) of the outside bathing media from 168 to 419 mM on specific phlorizin binding. These experiments were carried out at 8

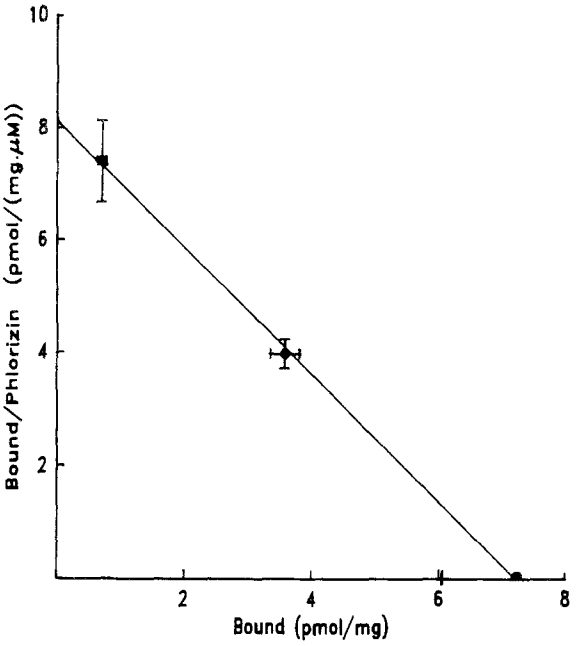

Fig. 5. Scatchard plot (as a function of phlorizin concentration) of the binding level reached at saturating sodium concentrations (*Bmn*). The apparent maximum number of binding sites *Bmn* at 0.095 and 0.9 μM phlorizin was found by extrapolation to infinite sodium in the modified Scatchard plots of the data in Fig. 4*b* and *c* (x axis intercepts) and the absolute number of binding sites (at infinite phlorizin) was measured experimentally as explained in the results. These values are displayed in this figure in a Scatchard plot as a function of phlorizin concentrations. The fit of Eq. (1) to the data yields an affinity constant of 0.89 μM and 7.23 pmol/mg for the maximum number of binding sites (*see* Discussion)

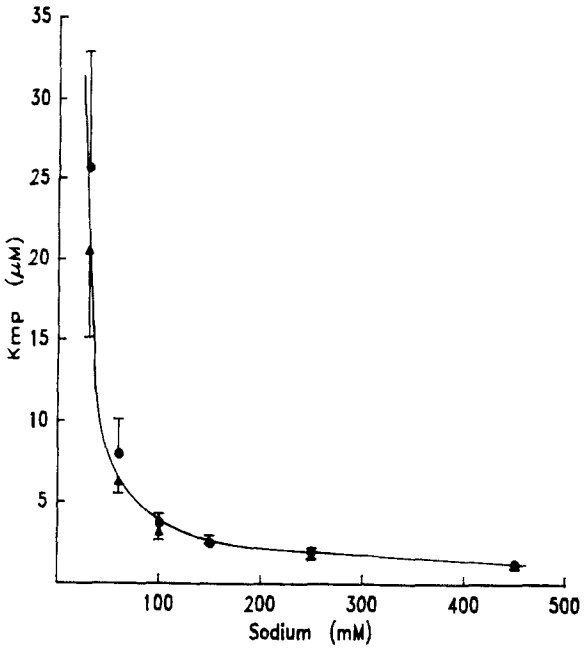

Fig. 6. Apparent affinity constant for phlorizin (K_{mp}) as a function of extracellular sodium. K_{mp} was calculated by transforming the data in Fig. 4*a* using Eq. (3). The triangles are the data calculated form the binding at 0.095 μM phlorizin, and the circles are those calculated from the data at 0.9 μM phlorizin. Values are shown ± SEM, $n = 3$

μM phlorizin in order to avoid effects related to changes in the membrane potential due to diffusion potentials.

Phlorizin Binding and Debinding Rates: Effects of Sodium and Membrane Potential

In preliminary experiments, we found that the rates for phlorizin binding and debinding at 37°C are too fast to allow accurate measurement. However, when the temperature of the assay is dropped to 1–2°C, it becomes possible to measure binding and debinding rates. Figure 9 shows that phlorizin debinding follows an exponential time course. Debinding is highly dependent on the presence of extracellular sodium, but is not affected by a change in the membrane potential. On the other hand, the rate of phlorizin binding is also highly dependent on sodium, but in addition, is dependent on the membrane potential (Fig. 10). Addition of 90 mM D-glucose lowered the binding rate at 270 mM Na^+, $\Delta\psi <$

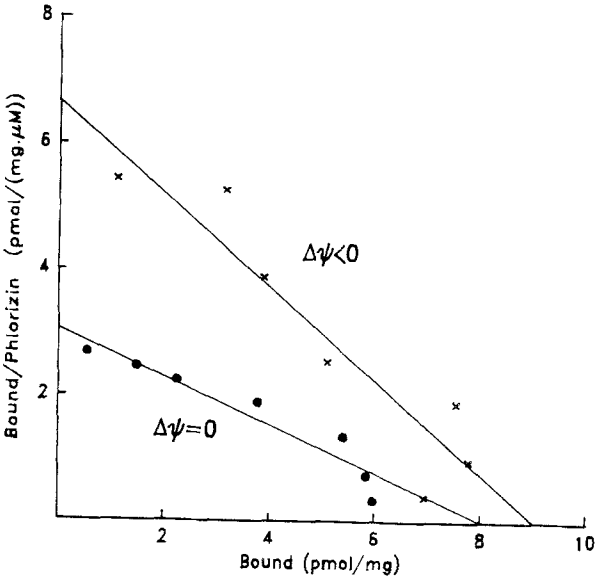

Fig. 7. Scatchard plot of specific phlorizin binding as a function of phlorizin at two membrane potentials. Cells were isolated in medium I and de-energized. At the initiation of binding, cells were diluted 1 : 10 in either medium II or VII (150 mM sodium) plus different concentrations of phlorizin (0.22–20 μM), and 1 mM phloretin. Negative (x) or near zero (●) membrane potentials were created using different potassium gradients and 40 μg/ml valinomycin. The Scatchard parameters for this experiment are: negative $\Delta\psi$: $K_{mp} = 1.35$ μM, $Bm = 9.0$ pmol/mg; zero $\Delta\psi$: $K_{mp} = 2.63$ μM, $Bm = 8.0$ pmol/mg

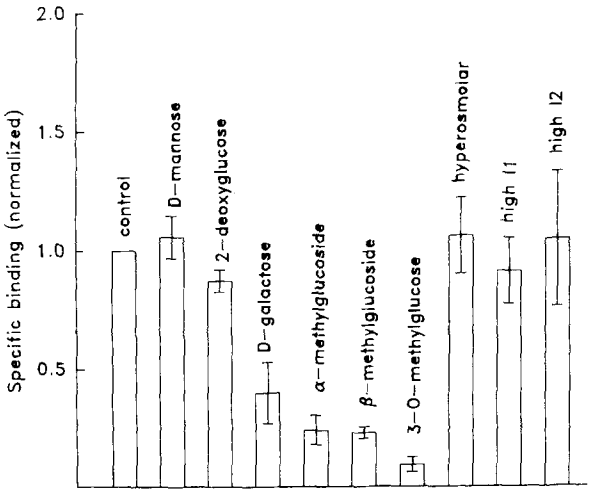

Fig. 8. Effect of the addition of sugars and changes in osmolarity and ionic strength on specific phlorizin binding. Cells were isolated in solution IX and were de-energized. Valynomycin (40 μg/ml) was added. At the start of the assay cells were diluted 1 to 10 such that the final concentrations were: 135 $NaNO_3$, 25 K-gluconate, 100 mannitol or 10 mannitol plus 90 D-glucose, 8 μM radioactive phlorizin, rotenone, ouabain and valinomycin plus: control: 90 mM mannitol (532 mOSM, I = 168 mM); 90 mM D-mannose; 90 mM 2-deoxyglucose; 90 mM D-galactose; 90 mM α-methylglucoside, 90 mM β-methylglucoside, 90 mM 3-O-methylglucose. Hyperosmolar: 540 mM mannitol (1150 mOSM, I = 168 mM); High $I1$: 225 Tris-cyclamate pH 7.4 plus 90 mM mannitol (1370 mOSM, I = 341 mM) and High $I2$: 225 TMA-gluconate plus 90 mM mannitol (1200 mOSM, I = 419 mM). The data shown are the average of two sets of three experiments ± SD. The data were normalized to the control in each experiment. The average value for the control is 12.87 ± 2.73 pmol/mg (mean ± SD, n = 6). The nonspecific binding was in the range 8–12 pmol/mg

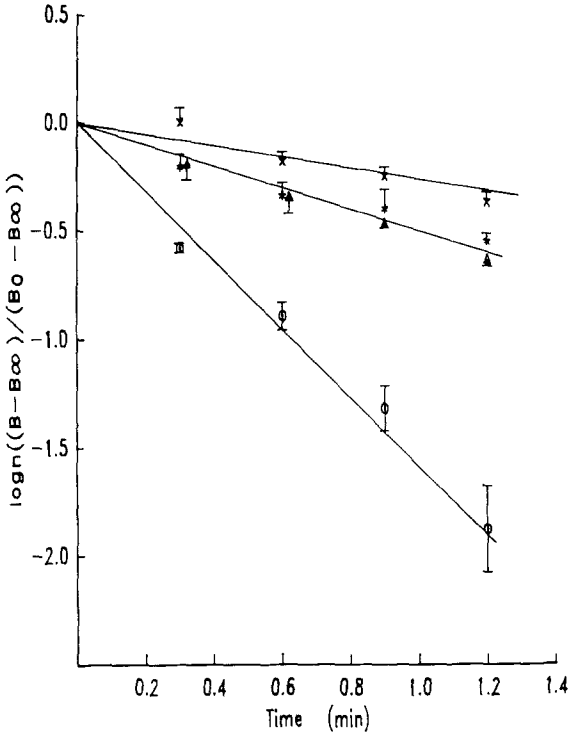

Fig. 9. Debinding of phlorizin: effect of sodium and the membrane potential. Cells were isolated and debinding was assayed at 1–2°C under conditions where more than 93% of the phlorizin bound was D-glucose inhibitable as explained in Materials and Methods. The membrane potential was controlled using potassium and valinomycin (cells were isolated in a medium containing 150 mM K-gluconate; *see* Materials and Methods). At the initiation of debinding cells were diluted 50-fold in media such that the final sodium concentration and membrane potentials were: (i) (x) $\Delta\psi < 0$; 299.4 mM Na^+ (medium X). (ii) (○) $\Delta\psi < 0$; 5.4 mM Na^+ (medium XI). (iii) (△) $\Delta\psi < 0$; 152.4 mM Na^+ (1 : 1 mixture of media X and XI), and (iv) (*) $\Delta\psi = 0$; 152.4 mM Na^+ (medium XII). All debinding solutions contained 30 μM unlabeled phlorizin. The rates of debinding were (mean ± SD, n = 3 in min^{-1}): (i) 299.4 Na^+: −0.29 ± 0.03; (ii) 5.4 Na^+: −1.54 ± 0.2; (iii) 152.4 Na^+, $\Delta\psi < 0$: −0.54 ± 0.03; (iv) 152.4 Na^+, $\Delta\psi = 0$: −0.48 ± 0.10. The average bound phlorizin at zero time was 1.37 ± 0.24 pmol/mg (mean ± SD)

0 to a level approximately equal to the level with no Na^+ (data not shown).

Discussion

The large surface-to-volume ratio of isolated intestinal epithelial cells allows measurement of initial rates of sugar uptake during intervals as large as 0–60 sec (Kimmich & Randles, 1981). The constancy of the rate of sugar influx over this interval indicates that the driving forces for the transport process are constant (sodium concentrations and membrane potential). We expected phlorizin binding to depend on these driving forces and hence to be constant in this time frame. In agreement with this premise, we find that D-glucose-inhibitable phlorizin binding to isolated enterocytes is constant for the period of 6–40 sec. This characteristic makes this preparation specially suited to the study of the kinetics of phlorizin binding.

Our data show that steady-state phlorizin binding is highly dependent on the presence of extracellular sodium, is altered by changes in the membrane potential, and is inhibited by actively transported sugars but not by sugars that cross the membrane by facilitated diffusion. These characteristics suggest that phlorizin is binding or being transported by the mucosal sodium-dependent transport system in agreement with observations derived from brush-

border vesicle preparations (Aronson, 1978; Turner & Silverman, 1981; Toggenburger et al., 1982).

Also in agreement with these studies we find that in contrast to the behavior of actively transported sugars: (i) phlorizin binding, at concentrations greater than the binding affinity, does not change if the osmolarity of the outside medium is changed; (ii) the rate of phlorizin dissociation is membrane-potential independent; (iii) the rate of association is highly dependent on $\Delta\psi$; and (iv) addition of excess cold phlorizin does not inhibit phlorizin debinding. Since steady-state accumulation of sugar is a function of medium osmolarity, and since efflux of sugar is $\Delta\psi$-dependent and inhibited by excess cold phlorizin (Kessler & Semenza, 1983; G. A. Kimmich, *unpublished observations*), these observations suggest that phlorizin is binding to the sugar carrier rather than being transported into the cells.

The excellent fit of specific phlorizin binding *vs.* phlorizin concentration to a rectangular hyperbola indicates the presence of a single homogeneous class of binding sites for phlorizin in this preparation in agreement with the Michaelian behavior of sugar fluxes on sugar concentration in chicken enterocytes (Restrepo & Kimmich, 1985*a*). This observation contrasts with studies in kidney where there are two distinct types of binding sites [2 sodium : 1 sugar proximal medullary transporter and a 1 sodium : 1 sugar cortex transporter (Turner & Moran, 1982*a*)]. The apparent affinity constant for phlorizin in our preparation is sodium dependent in agreement with the data for kidney cortex (Turner & Silverman, 1981).

However, it is the sodium dependence of specific phlorizin binding which provides a wealth of kinetic information with implications for transport mechanism. For instance, Fig. 4 shows that the activation of phlorizin binding by sodium is fit by a concave down curve rather than by a straight line on a Scatchard plot in contrast with the data reported by Turner and Silverman (1981) in dog kidney cortex and Turner and Moran (1982*b*) in rabbit kidney cortex. This evidence, together with the directly measured sodium/sugar coupling stoichiometry of 2 : 1 (Kimmich & Randles, 1980, 1984) for the chicken intestinal transporter is highly suggestive (but not a proof) of a stoichiometry of 2 sodiums per phlorizin bound.

Another important feature of the data in Fig. 4 is that the level of phlorizin binding reached at saturating sodium concentrations is phlorizin dependent. This rules out all ordered binding models in which the last step involves the binding of sodium since in these models high concentrations of sodium

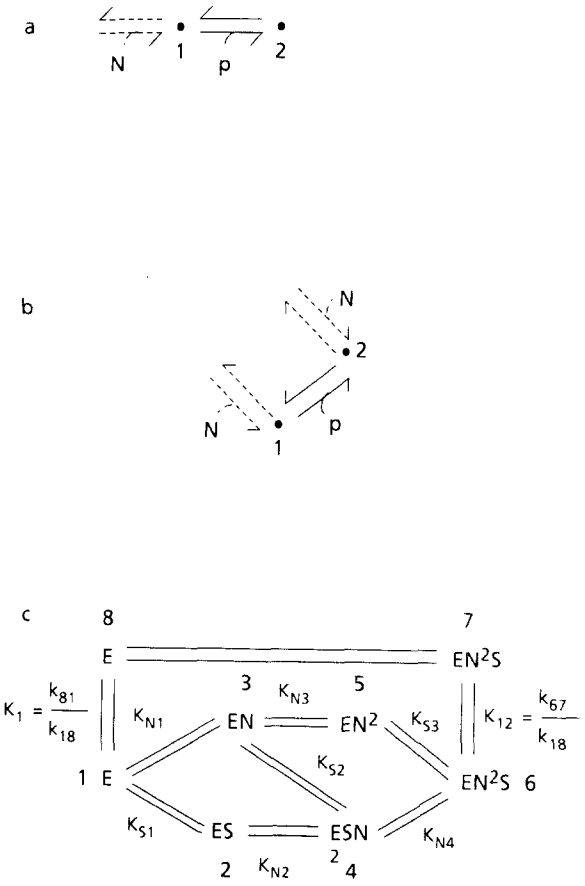

Fig. 10. Phlorizin association rate: effect of sodium and the membrane potential. Cells were isolated and binding of 0.1 μM phlorizin was assayed at 1–2°C as explained in Materials and Methods. The membrane potential was controlled by using potassium and valinomycin. At the initiation of the binding assay cells were diluted 1 : 10 in different solutions. The incubation conditions were (final concentrations in mM): (i) (●) 270 Na^+, $\Delta\psi < 0$ (medium XIII); (ii) (▲) 270 Na^+, $\Delta\psi = 0$ (medium XIV); (iii) (x) No Na^+ (medium XV). (*a*) Average from three experiments ± SEM. The data have been normalized and corrected for zero time binding or trapping as discussed in Materials and Methods. The absolute binding level at 270 mM Na^+ $\Delta\psi < 0$ and $t = 1.2$ min was in the range 108 to 244 fmol/mg (corrected for the intercept) and the intercept ranged from 20 to 38 fmol/mg. (*b*) Results from one experiment showing an amplified time scale (the data for *b* were not corrected for zero time binding or trapping and were not normalized)

can trap the carrier in the phlorizin/sodium loaded form(s) (*see* Appendix). In ordered models that involve phlorizin as the last binding step, sodium can only draw the carrier to the sodium-loaded phlorizin-free form which will then equilibrate with the phlorizin-loaded form in accord with the phlorizin concentration and the true affinity contrast for phlorizin (*Kp*). Random models also exhibit this behav-

ior (*see* Appendix). Hence, the data in Fig. 4 rules out the bibi ordered phlorizin/sodium model and the terter ordered phlorizin/sodium/sodium as well as the ordered terter model involving sodium/phlorizin/sodium.

All remaining models predict that at saturating sodium concentrations the apparent affinity constant for phlorizin (K_{mp}) becomes equal to the true affinity constant for phlorizin (Kp). This is illustrated in Fig. 6 in which the data in Fig. 4 was transformed using Eq. (3) to display the sodium concentration dependence of K_{mp}. As shown, K_{mp} decreases with increasing sodium and the curve approaches an assymptote at high sodium at a value of about 0.9 μM. In the Appendix it is also shown that (for the models that have not been ruled out) at saturating sodium, the binding levels should follow Eq. (1) with K_{mp} replaced by Kp and hence, when displayed in a Scatchard format, the data should fall on a straight line. Figure 5 shows that the data at saturating sodium concentrations does indeed fit a straight line in a Scatchard plot and a linear regression gives 0.89 μM for the true affinity constant for this particular set of experiments.

The association and dissociation rates for phlorizin have been shown to be sodium dependent in rabbit kidney (Aronson, 1978), dog kidney cortex (Turner & Silverman, 1981), and rabbit intestine (Toggenburger et al., 1982). The large sodium dependence for phlorizin association indicates that in the presence of sodium, phlorizin association is a preferred ordered event with sodium binding first being the preferred pathway. The sodium dependence of phlorizin dissociation rules out the ordered terter sodium/sodium/phlorizin as a possible model and indicates that in the absence of sodium, dissociation of sodium first is the preferred pathway. This agrees with evidence from sodium self exchange through the sodium-dependent transporter which indicates that (in the absence of sodium inside) sodium dissociation is the preferred pathway at the intracellular interface (Kimmich & Randles, 1984). The sodium dependence of both sodium dissociation and association and the phlorizin dependence of binding levels at saturating sodium indicate that phlorizin and sodium bind to the transporter in a random fashion, but that the sodium first route is favored over the phlorizin first route for association. The sodium dependence of the rates also indicates that sodium increases the binding affinity for sugar (as explained by Aronson, 1978).

In view of evidence about the possibility that sodium dependent systems may share a common subunit that couples the flux of sodium to the flux of other solutes in *Escherichia coli* (Zilberstein, Ophir, Padan & Schuldiner, 1982), it is interesting to point out that a random binding model would agree with a multisubunit arrangement in which the sodium binding site is in a different subunit from the sugar (phlorizin) binding site. A random sodium/phlorizin binding mechanism (but with a 1 : 1 stoichiometry) was proposed by Aronson (1978) for rabbit kidney cortex and by Turner and Silverman (1981) for dog kidney cortex. In the kidney cortex system the proposed phlorizin/sodium binding stoichiometry is supported by firm measurements of the sugar/sodium stoichiometry. Hence, it may be that the difference between the kidney cortex transporter and the chicken intestinal transporter is that the coupling stoichiometries are different with similar binding mechanisms. Comparison of the chicken intestinal transporter with the rabbit intestinal transporter is less clear. The experimental observations reported by Toggenburger et al. (1982) could be explained by our proposed model.

The $\Delta\psi$ dependence of the apparent affinity constant for phlorizin and of the association constant, and the $\Delta\psi$ independence of phlorizin dissociation indicate that if translocation is the membrane potential-dependent step, the free carrier must be negatively charged (Toggenburger et al., 1982; Aronson, 1978, 1984). Alternatively, the observed membrane potential dependence can also be due to potential-dependent sodium binding (Restrepo & Kimmich, 1985*b*). A model of this type, in which the first sodium must traverse part of the electric field to reach its binding site but the second sodium binds close to the extracellular interface, would exhibit a large $\Delta\psi$ dependence for the association constant and a small $\Delta\psi$ dependence for the dissociation constant.

Since phlorizin is a competitive inhibitor for sugar and since the sodium and membrane potential behavior of sugar influx resembles that of phlorizin, it is probable that the binding mechanisms for both solutes to the sodium-dependent transporter are alike. In an earlier paper (Restrepo & Kimmich, 1985*a*), we had favored an ordered terter model with binding order sodium/sugar/sodium over the random binding model for sugar because of observations on sodium self exchange through the transporter, which suggest that debinding is ordered (sodium debinding first). Even though at low sodium a particular debinding route is favored, the data taken in total suggest that the binding order is random and that the random 2 sodium to 1 sugar mechanism should be considered as the most likely candidate for sodium-sugar cotransport in chicken intestine. The random binding model for sugar transport provides a theoretical basis for explaining the experimentally determined [sodium], [sugar], and membrane potential dependence for sodium-dependent

sugar fluxes (Restrepo & Kimmich, 1985*a*,*b*; *also see* Appendix).

We acknowledge the excellent technical assistance by Mrs. Geraldine Bebernitz. This work was supported by the National Institute of Arthritis, Metabolism and Digestive Diseases Grant AM-15365.

References

Aronson, P.S. 1978. Energy-dependence of phlorizin binding to isolated renal microvillus membranes. *J. Membrane Biol.* **42:**81–98

Aronson, P.S. 1984. Electrochemical driving forces for secondary active transport: Energetics and kinetics of Na^+–H^+ exchange and Na^+-glucose cotransport. *In:* Electrogenic Transport: Fundamental Principles and Physiological Implications. M.P. Blaustein and M. Lieberman, editors. pp. 49–70. Raven, New York

Carter-Su, C., Kimmich, G.A. 1979. Membrane potentials and sugar transport by ATP-depleted intestinal cells: Effect of anion gradients. *Am. J. Physiol.* **6(1):***C*67–*C*74

Crane, R.K. 1960. Intestinal absorption of sugars. *Physiol. Rev.* **40:**784–825

Gornall, A., Bardawill, C., David, M. 1979. Determination of serum protein by means of the biuret reaction. *J. Biol. Chem.* **177:**751–758

Hill, T.L. 1977. Free Energy Transduction in Biology. Academic, New York

Kessler, M., Semenza, G. 1983. The small intestinal Na^+, D-glucose cotransporter: An asymmetric gated channel (or pore) responsive to $\Delta\psi$. *J. Membrane Biol.* **76:**27–56

Kessler, M., Tannenbaum, V., Tannenbaum, C. 1978. A simple apparatus for performing short-time (1–2 sec) uptake measurements in small volumes; Its application to D-glucose transport studies in brush-border vesicles from rabbit jejunum and ileum. *Biochem. Biophys. Acta* **509:**348–359

Kimmich, G.A. 1970. Preparation and properties of mucosal epithelial cells isolated from small intestine of the chicken. *Biochemistry* **9:**3659–3668

Kimmich, G.A. 1973. Coupling between Na^+ and sugar transport in small intestine. *Biochim. Biophys. Acta* **300:**31–78

Kimmich, G.A., Randles, J. 1976. 2-Deoxyglucose transport by intestinal epithelial cells isolated from the chick. *J. Membrane Biol.* **27:**363–379

Kimmich, G.A., Randles, J. 1980. Evidence for an intestinal Na^+ : sugar transport coupling stoichiometry of 2.0. *Biochim. Biophys. Acta* **596:**439–444

Kimmich, G.A., Randles, J. 1981. α-Methylglucoside satisfies only Na^+-dependent transport system of intestinal epithelium. *Am. J. Physiol.* **241:***C*227–*C*232

Kimmich, G.A., Randles, J. 1984. Sodium-sugar coupling stoichiometry in chick intestinal cells. *Am. J. Physiol.* **247:***C*74–*C*82

King, E., Altman, C. 1956. A schematic method of deriving the rate laws for enzyme-catalyzed reactions. *J. Phys. Chem.* **60:**1375–1378

Montrose, M., Bebernitz, G., Kimmich, G.A. 1985. Evaluation of ion gradient-dependent H^+ transport systems in isolated enterocytes from the chick. *J. Membrane Biol.* **88:**55–66

Restrepo, D., Kimmich, G.A. 1985*a*. Kinetic analysis of the mechanism of intestinal Na^+-dependent sugar transport. *Am. J. Physiol.* **248:***C*498–*C*509

Restrepo, D., Kimmich, G.A. 1985*b*. The mechanistic nature of the membrane potential dependence of sodium-sugar cotransport in small intestine. *J. Membrane Biol.* **87:**159–172

Segel, I.H. 1975. Enzyme Kinetics. pp. 846–883. John Wiley & Sons, New York

Tannenbaum, C., Toggenburger, G., Kessler, M., Rothstein, A., Semenza, G. 1977. High-affinity phlorizin binding to brush-border membranes from small intestine: Identity with (a part of) the glucose transport system, dependence on the Na^+ gradient, partial purification. *J. Supramol. Struct.* **6:**519

Toggenburger, G., Kessler, M., Rothstein, A., Semenza, G., Tannenbaum, C. 1978. Similarity in effects of Na^+ gradients and membrane potentials on D-glucose transport by, and phlorizin binding to, vesicles derived from brush borders of rabbit intestinal mucosal cells. *J. Membrane Biol.* **40:**269–290

Toggenburger, G., Kessler, M., Semenza, G. 1982. Phlorizin as a probe of the small-intestinal Na^+, D-glucose cotransporter. A model. *Biochim. Biophys. Acta* **688:**557–571

Turner, R.J., Moran, A. 1982*a*. Further studies of proximal tubular brush border membrane D-glucose transport heterogeneity. *J. Membrane Biol.* **70:**37–45

Turner, R.J., Moran, A. 1982*b*. Stoichiometric studies of the renal cortical brush border membrane D-glucose transporter. *J. Membrane Biol.* **67:**73–80

Turner, R.J., Silverman, M. 1980. Testing carrier models of cotransport using the binding kinetics of nontransported competitive inhibitors. *Biochim. Biophys. Acta* **596:**272–291

Turner, R.J., Silverman, M. 1981. Interaction of phlorizin and sodium with the renal brush-border membrane D-glucose transporter: Stoichiometry and order of binding. *J. Membrane Biol.* **58:**43–55

Zilberstein, D., Ophir, I.J., Padan, E., Schuldiner, S. 1982. Na^+ gradient coupled porters of *Escherichia coli* share a common subunit. *J. Biol. Chem.* **257:**3692–3696

Received 17 July 1985

Appendix

Theoretical Analysis

Phlorizin Binding

In order to carry out the analysis of the kinetic data, we solved the binding equations using the King-Altman method (King & Altman, 1956; Segel, 1975; Hill, 1977). In this Appendix, we will explain, in terms of King-Altman theory, the results relevant to this article. The kind of binding models that we consider are those that bind both phlorizin and sodium with 1 : 1 and 2 : 1 phlorizin/sodium stoichiometries. For all cases, the form of the binding equation as a function of phlorizin and sodium is

$$B = BmNum(P,N)/Den(P,N) \qquad \text{(A1)}$$

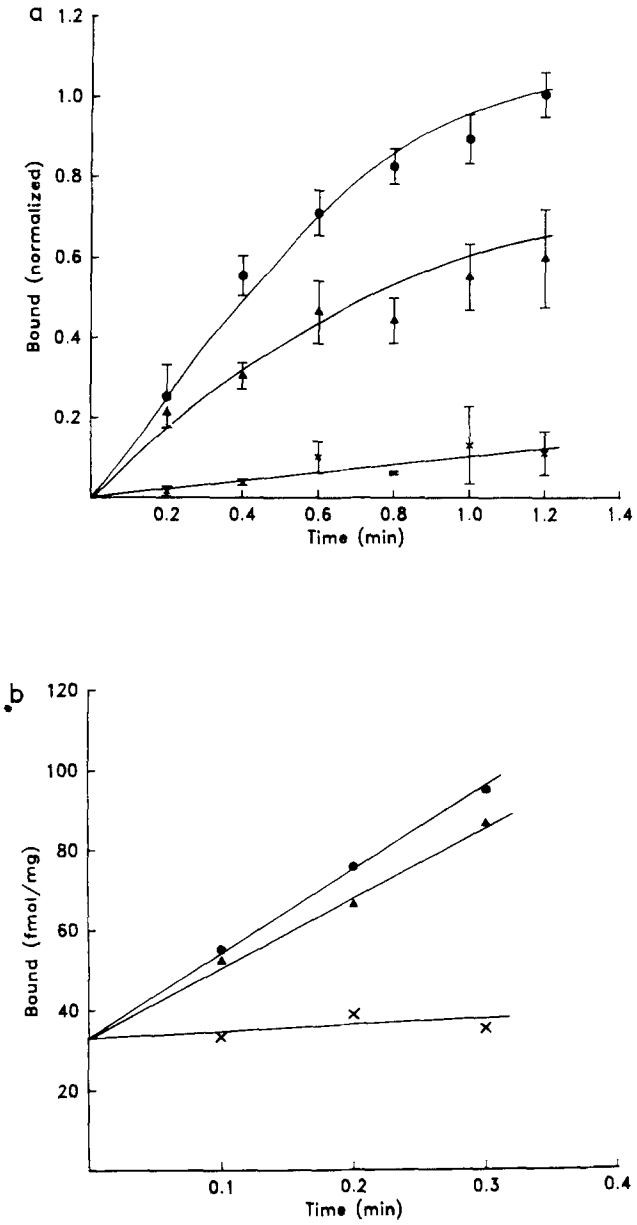

Fig. 11. Diagrams of binding and transport models considered. (*a*) Ordered binding models in which phlorizin is the last binding step. The different states of the transport system are labeled with numbers. (*b*) Random binding models. Shown are the states whose King-Altman terms will rule the binding equation at high sodium. (*c*) 2 sodium : 1 sugar terter random order model

where P and N are sodium and phlorizin concentrations, Bm is the absolute maximum number of binding sites, and Num and Den are polynomials in terms of P and N.

1) Ordered binding models in which sodium is the last ligand to bind have a binding level at saturating sodium (Bmn) independent of phlorizin concentrations (P).

To find Bmn, it is necessary to find the terms in the denominator and numerator of the binding equation that are of highest order in sodium. If the last binding step involves sodium binding, the term with highest order in sodium in the denominator and numerator will be the King-Altman term corresponding to the totally loaded form of the phlorizin/sodium receptor. Since this term appears in both denominator and numerator, at saturating sodium the terms will cancel and the number of binding sites at saturating sodium (Bmn) will be equal to Bm.

2) For ordered models in which phlorizin is the last ligand to bind, Bmn depends on phlorizin as

$$B = BmP/(Kp + P) \tag{A2}$$

where Kp is the true affinity for phlorizin to the transporter.

For these models the last two steps are a sodium binding step followed by a phlorizin binding step. At saturating sodium, the two terms with highest order in sodium will be those King-Altman terms that correspond to binding states to the right of the last sodium binding step. In Fig. 11*a* we have labeled these two states as *1* and *2*. Of these two steps only 2 will appear in the numerator. The mathematical form for the two King-Altman terms corresponding to these states is: for 2, $C(N)k_{12}P$; and for 1, $C(N)k_{21}$. Where $C(N)$ is a function of sodium (N). Hence, the binding equation at saturating sodium will be Eq. (A2) with $Kp = k_{21}/k_{12}$.

For the random models, the argument is similar except that the diagram instead of looking like Fig. 11*a* is as depicted in Fig. 11*b*. In this case, at saturating sodium states, 1 and 2 are the only ones left. Using the same reasoning as above, we find that the binding equation at saturating sodium is given by Eq. (A2).

Random Binding 2 Sodium : 1 Sugar Terter Model: Some Remarks on the Membrane Potential and Sodium Dependence of the Maximum Velocity for Sugar when Translocation is Rate Limiting

In an earlier paper (Restrepo & Kimmich, 1985*b*) we found that the maximum velocity for sugar transport as a function of sugar is membrane-potential independent and that the K_{ms} is highly membrane-potential dependent. We analyzed the implications of these results in terms of the ordered binding terter NSN model when translocation is rate limiting and concluded that the model in which translocation is membrane-potential dependent and the free carrier is neutral could be discarded. The corresponding analysis for the random 2 sodiums : 1 sugar model is as follows:

The equation that describes sugar flux for this model was solved in Restrepo and Kimmich (1985*a*). The maximum velocity J_{ms} (i.e., the flux at saturating sugar) is given by

$$J_{ms} = \rho k_{67}N^2/(K_{N4}K_{N2} + NK_{N4} + (1 + (K_{12}/K_1))N^2 \tag{A3}$$

where the rate constants are defined according to Fig. 11*c*. If the free carrier is neutral, the membrane potential-dependent term will be the rate constant k_{67}. In order for J_{ms} to be membrane-potential independent (as shown experimentally in Restrepo and Kimmich (1985*a*), the term $K_{12}/K_1(N^2)$ must be much larger than all other terms in the denominator. However, in this case, J_{ms} would also be sodium independent contrary to experimental evidence presented by us (Restrepo & Kimmich, 1985*a*,*b*). Hence, the model where translocation is the membrane potential-dependent step and the free carrier is not charged is not an appropriate candidate for sodium-dependent sugar transport.